ARCHIVES OF ELECTRICAL ENGINEERING VOL. 60(3), pp. 331-348 (2011)

DOI 10.2478/v10171-011-0029-0

Hamiltonian model of electromechanical actuator in natural reference frame. Part II: Equations and simulations

WOJCIECH BURLIKOWSKI

Department of Mechatronics, Faculty of Electrical Engineering
Silesian University of Technology
Akademicka 10a, 44-100 Gliwice, Poland
e-mail:wojciech.burlikowski@polsl.pl

(Received: 11.03.2011, revised: 26.05.2011)

Abstract: In the paper a novel mathematical model of electromechanical actuator is presented. It is based on application of Hamiltonian equations in the description of electromechanical energy conversion. It results in employment of flux linkages as state variables in the state space equations. For simplicity only a 3-phase wye connected stator winding without a neutral wire is considered in detail. The procedure can be generalised to any number of phases. Topology-based approach is used in the model implementation. Procedures for evaluation of all quantities (currents, energy/coenergy, electromagnetic torque) present in model equations are described. Eddy currents and hysteresis phenolmenon are neglected in formulation of the model to enable application of state-space description.
Key words: electromechanical actuators, reluctance motor, Hamiltonian equations

1. Introduction

Modern synchronous drives both with reluctance motors (SynRM) and permanent magnet motors (PMSM, BLDC) employ very sophisticated control schemes [3]. It enables their application in the most complicated servo-drives and positioning systems. Therefore, in their design and optimisation a very accurate mathematical models are necessary. Nowadays such models are based on field-circuit discrete modellers using Finite Element Method (FEM) coupled with circuit solvers like Simplorer and Simulink [14, 20, 29]. There appear attempts to apply field-circuit model for control design [14, 20, 21]. Both direct and indirect coupling between FEM and circuits is employed [20, 29, 31, 36, 42].

On the contrary, in the design of control algorithms commonly-used circuit models are mostly very simple, only slightly different from original Park *dq0* model proposed around 1920s [33]. Therefore it is very difficult to account for certain phenomena (e.g. MMF harmonics, slotting effects in SynRM or cogging torques in PMSM/BLDC) in the designing stage of the drive control algorithm. Their influence (e.g. vibrations, parasitic torques) is commonly treated as an outer disturbance. Electromechanical actuator circuit models which account for such the phenomena are very complicated which makes them difficult to apply for designing electric drives, although such attempts are made [24, 39]. It is especially important for sensorless drives [3, 4, 32].

In the paper a novel mathematical model of electromechanical actuator is presented. It is based on application of Hamiltonian equations in description of electromechanical energy conversion which results in employment of flux linkages as state variables in the state-space equations [37, 39]. For simplicity of description only a 3-phase wye-connected stator winding without a neutral wire is considered in details. This connection scheme is the most important from practical viewpoint [3, 4]. The procedure can be extended to any number of phases and an arbitrary connection schema. In formulation of the model the eddy currents and hysteresis phenomenon were neglected to enable application of Hamiltonian formalism [37].

The model is formulated in natural (phase) reference frame. It is shown that for a 3-phase wye-connected stator winding without neutral wire a 2-phase equivalent generalised circuit can be obtained. The voltage circuit equations are established using Kirchhoff's equations with flux linkages as state variables which is a result of Hamiltonian approach. The most important problem arising in this approach is evaluation of currents as function of flux linkages in multivariable space [7, 8, 39]. The proposed solution is based on the triangulation of databases (obtained using FEM [7, 8] or a measurement [42]) and application of local linear (affine) homeomorphism between the spaces of variables [P. I] [19] (space of currents and space of flux linkages). In algebraic topology this approach is defined as simplical approximation [2, 16, 40, 44]. Similar approach is used in description of non-linear circuits and networks [9, 10, 23, 41].

2. An electromechanical actuator state space model using Hamiltonian equations

Application of Hamiltonian equations in analysis of electromechanical actuators is very uncommon although it is equivalent to Lagrange equations [35, 37, 39]. In physics (e.g. relativistic mechanics [43]) the Hamiltonian equations are even more popular than Lagrange equations [10, 22]. In case of electromechanical actuators potential advantage of Hamiltonian description is the canonical form of these equations. The state of the system can be uniquely described using the so-called Hamiltonian H [22, 39]:

$$H = E_{mag} + E_k + E_p. \tag{1}$$

where E_{mag} – magnetic field energy, E_k – kinetic energy of mechanical part of the system, E_p – potential energy of the system. When the machine with m insulated phase windings $A, B, \ldots, M$ is considered the magnetic field energy can be described by the following formula [39]:

$$E_{mag}(\varphi, \mathbf{\Psi}_{ph}) = \sum_{j=A}^{M} \int_{0}^{\psi_j} i_j\left(\varphi, \psi_A, \ldots, \psi_j, 0, \ldots, 0\right) \mathrm{d}\psi_j \,, \tag{2}$$

where φ – angular position of the rotor (Fig. 2), $\mathbf{\Psi}_{ph} = [\psi_A, \ldots, \psi_j \ldots, \psi_M]^T$ – vector of phase flux linkages, $\boldsymbol{i}_{ph} = [i_A, \ldots, i_j, \ldots, i_M]^T$ – vector of phase currents. Equation (2) can also be written in the more general form for arbitrary variation of the flux linkages [37]:

$$E_{mag}(\varphi, \mathbf{\Psi}_{ph}) = \int_{\mathbf{0}}^{\mathbf{\Psi}_{ph}} \boldsymbol{i}_{ph} \cdot \mathrm{d}\mathbf{\Psi} \Bigg|_{\varphi=\mathrm{const}} = \int_{\mathbf{0}}^{\mathbf{\Psi}_{ph}} \mathbf{i}_{ph}^T \, \mathrm{d}\mathbf{\Psi} \Bigg|_{\varphi=\mathrm{const}}, \tag{3}$$

where two forms of vector dot product representation used in this paper, vector and matrix, are shown.

When the w holonomic constraints are imposed on the system the number of degrees of freedom can be reduced [37, 43]. The state of the system is then described by $N+1$ independent canonical equations where $N = m\text{-}w$:

$$\frac{\mathrm{d}}{\mathrm{d}t}\lambda_j + \frac{\partial H}{\partial q_j} - Q_j = 0 \tag{4}$$

$j \in \{1, \ldots, N+1\}$ with additional $N+1$ equations defining relationship between generalised momenta and generalised velocities:

$$\frac{\mathrm{d}}{\mathrm{d}t} q_j = \frac{\partial H}{\partial \lambda_j}, \tag{5}$$

where $\boldsymbol{\lambda} = [K, \psi_1, \ldots, \psi_j, \ldots, \psi_N]^T = [K, \mathbf{\Psi}^T]^T$ – vector of generalised momenta of the system, K – angular momentum, $\mathbf{\Psi}$ – vector of generalised flux linkages, $\boldsymbol{q} = [\varphi, q_1, \ldots, q_j, \ldots q_N]^T = [\varphi, \boldsymbol{q}_e^T]^T$ – vector of generalised coordinates of the system, $\boldsymbol{q}_e$ – vector of generalised electrical coordinates of the system (charges), Q_j – j-th component of generalised non-potential force acting in the system, $\dot{\boldsymbol{q}} = [\omega, i_1, \ldots, i_j, \ldots, i_N]^T = [\omega, \boldsymbol{i}^T]^T$ – vector of generalised velocities, ω – angular velocity, $\boldsymbol{i}$ – vector of generalised electrical velocities (currents).

In the analysed cases such constraints are result of a connection scheme (e.g. wye without neutral wire). When there are no potential energy elements in the system the Hamiltonian can be re-written into a simpler form:

$$H(\varphi, K, \mathbf{\Psi}) = E_{mag}(\varphi, \mathbf{\Psi}) + \frac{K^2}{2J}, \tag{6}$$

$$E_{mag}(\varphi, \mathbf{\Psi}) = \int_{\mathbf{0}}^{\mathbf{\Psi}} \boldsymbol{i} \cdot \mathrm{d}\mathbf{\Psi} = \int_{\mathbf{0}}^{\mathbf{\Psi}} \boldsymbol{i}^T \mathrm{d}\mathbf{\Psi}. \tag{7}$$

There exists a relationship connecting energy and coenergy of the magnetic field defined by Legendre transformation [22, 37]:

$$E_{mag}(\varphi, \mathbf{\Psi}) + E_{cm}(\varphi, \boldsymbol{i}) = \mathbf{\Psi}^T \boldsymbol{i}, \tag{8}$$

where the coenergy is:

$$E_{cm}(\varphi, \boldsymbol{i}) = \int_{\mathbf{0}}^{\boldsymbol{i}} \boldsymbol{\Psi} \cdot \mathrm{d}\boldsymbol{i}\,. \tag{9}$$

The coenergy is much more popular in the description of electromechanical actuators as it is present in the Lagrange equations [37, 39, 43].

In matrix form the equations (4), (5) can be written separately for electric and mechanical degrees of freedom:

$$\begin{gathered}
\frac{\mathrm{d}\boldsymbol{\Psi}}{\mathrm{d}t} = \boldsymbol{u} - \boldsymbol{R}\,\boldsymbol{i}(\varphi, \boldsymbol{\Psi}) \\
\frac{\mathrm{d}K}{\mathrm{d}t} = T_e - T_m \\
\frac{\mathrm{d}\varphi}{\mathrm{d}t} = \frac{K}{J} \\
T_e = -\frac{\partial E_{mag}(\varphi, \boldsymbol{\Psi})}{\partial \varphi} = \frac{\partial E_{cm}(\varphi, \boldsymbol{i})}{\partial \varphi}\,,
\end{gathered} \tag{10}$$

where $\boldsymbol{i}(\varphi, \boldsymbol{\Psi})$ is the function that defines currents in terms of rotor angular position φ and generalised electric momenta $\boldsymbol{\Psi}$ (flux linkages); $\boldsymbol{u}$ – generalised external electric forces (voltages); $\boldsymbol{R}$ – resistance matrix; T_e – electromagnetic torque; T_m – mechanical load torque, J – moment of inertia. Equation set (10) can be presented in a form of block diagram shown in Fig. 1.

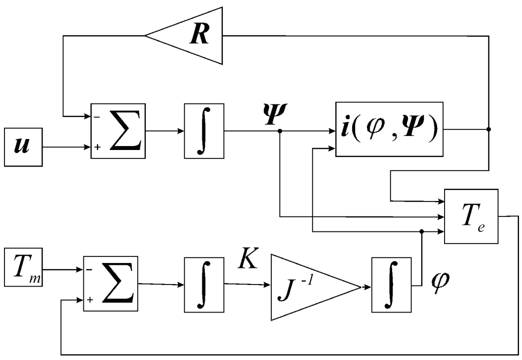

Fig. 1. Block diagram of electromechanical actuator mathematical model using Hamiltonian equations (HMEA)

3. Description of ‘electrical state-space’ using Kirchhoff’s equations

Standard connection schemas for a 3-phase ($m = 3$) reluctance motor and their equivalent circuit representations are shown depicted in Fig. 2. For each of them the Hamiltonian electric equation in (10) can be obtained using Kirchhoff’s equations.

Therefore, for each schema its voltage equation can be written in two different forms:

- Kirchhoff’s form – using phase variable description; denoted by (K.),
- Hamiltonian form – using generalised variable description; denoted by (H.).

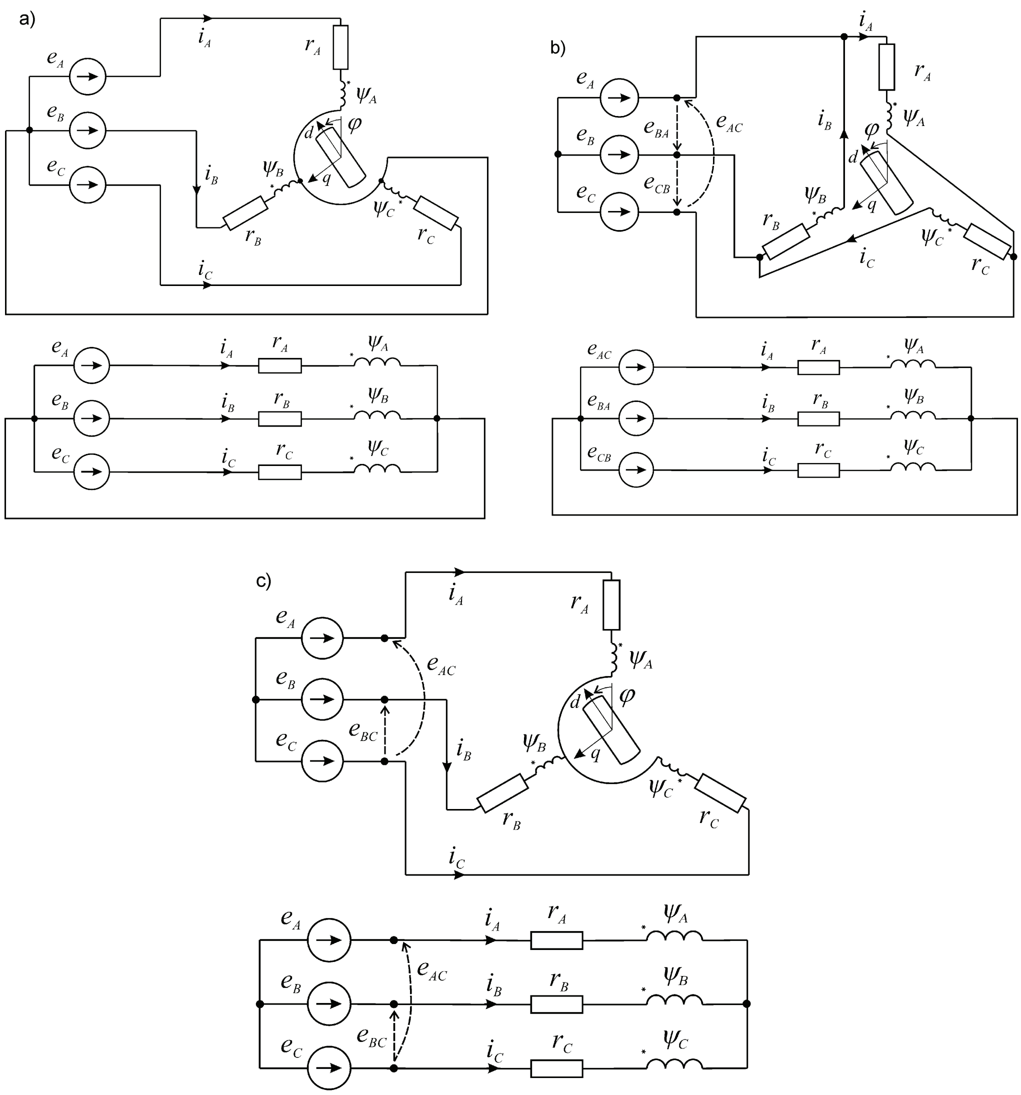

Fig. 2. Schematic representations of the reluctance motor and their equivalent circuits for different connection schemas a) wye with neutral wire, b) delta, c) wye without neutral wire

The voltage equations are:

- for wye with neutral wire ($w = 0$, $N = m$)

$$\overset{\text{(K.)}}{\begin{bmatrix} e_A \\ e_B \\ e_C \end{bmatrix} = \frac{\mathrm{d}}{\mathrm{d}t}\begin{bmatrix} \psi_A \\ \psi_B \\ \psi_C \end{bmatrix} + \begin{bmatrix} r_A & 0 & 0 \\ 0 & r_B & 0 \\ 0 & 0 & r_C \end{bmatrix}\begin{bmatrix} i_A \\ i_B \\ i_C \end{bmatrix}} \overset{\text{(H.)}}{\begin{bmatrix} u_1 \\ u_2 \\ u_3 \end{bmatrix} = \frac{\mathrm{d}}{\mathrm{d}t}\begin{bmatrix} \psi_1 \\ \psi_2 \\ \psi_3 \end{bmatrix} + \begin{bmatrix} r_1 & 0 & 0 \\ 0 & r_2 & 0 \\ 0 & 0 & r_3 \end{bmatrix}\begin{bmatrix} i_1 \\ i_2 \\ i_3 \end{bmatrix}}, \tag{11}$$

- for delta ($w = 0$, $N = m$)

$$\text{(K.)}\quad \begin{bmatrix} e_{AC} \\ e_{BA} \\ e_{CB} \end{bmatrix} = \frac{\mathrm{d}}{\mathrm{d}t}\begin{bmatrix} \psi_A \\ \psi_B \\ \psi_C \end{bmatrix} + \begin{bmatrix} r_A & 0 & 0 \\ 0 & r_B & 0 \\ 0 & 0 & r_C \end{bmatrix}\begin{bmatrix} i_A \\ i_B \\ i_C \end{bmatrix} \qquad \text{(H.)}\quad \begin{bmatrix} u_1 \\ u_2 \\ u_3 \end{bmatrix} = \frac{\mathrm{d}}{\mathrm{d}t}\begin{bmatrix} \psi_1 \\ \psi_2 \\ \psi_3 \end{bmatrix} + \begin{bmatrix} r_1 & 0 & 0 \\ 0 & r_2 & 0 \\ 0 & 0 & r_3 \end{bmatrix}\begin{bmatrix} i_1 \\ i_2 \\ i_3 \end{bmatrix}, \tag{12}$$

- for wye without neutral wire ($w = 1$, $N = m - 1$)

$$\begin{aligned} &\text{(K.)}\quad \begin{bmatrix} e_{AC} \\ e_{BC} \end{bmatrix} = \frac{\mathrm{d}}{\mathrm{d}t}\begin{bmatrix} \psi_{AC} \\ \psi_{BC} \end{bmatrix} + \begin{bmatrix} r_A + r_C & r_C \\ r_C & r_B + r_C \end{bmatrix}\begin{bmatrix} i_A \\ i_B \end{bmatrix} \\ &\text{(H.)}\quad \begin{bmatrix} u_1 \\ u_2 \end{bmatrix} = \frac{\mathrm{d}}{\mathrm{d}t}\begin{bmatrix} \psi_1 \\ \psi_2 \end{bmatrix} + \begin{bmatrix} r_{11} & r_{12} \\ r_{21} & r_{22} \end{bmatrix}\begin{bmatrix} i_1 \\ i_2 \end{bmatrix}. \end{aligned} \tag{13}$$

In case of two first connection schemas (wye with neutral wire, delta) the number of degrees of freedom is unchanged and the resistance matrices are diagonal and equal to the phase resistance matrix.

The generalised variables in case of wye connection with neutral wire are same with phase variables (11).

In case of the delta connection the generalised external electric forces u_1, u_2, u_3 are line-to-line voltages e_{AC}, e_{BA}, e_{CB} whilst all the other generalised variables are phase variables (12).

The most interesting case from practical point of view is wye without neutral wire. Application of Hamiltonian approach (13) shows that:

- flux linkages ψ_{AC}, ψ_{BC} – line-to-line flux linkages being linear combinations of phase flux linkages $\psi_{AC} = \psi_A - \psi_C$, $\psi_{BC} = \psi_B - \psi_C$ are generalised electric momenta ψ_1, ψ_2 [8, 32],
- voltages e_{AC}, e_{BC} – line-to-line voltages being linear combinations of phase voltages $e_{AC} = e_A - e_C$, $e_{BC} = e_B - e_C$ are generalised external electric forces u_1, u_2,
- currents i_A, i_B – being simultaneously the loop and phase currents are generalised electric velocities i_1, i_2,
- the resistance matrix is symmetric but non-diagonal.

The 3-phase wye connected stator winding without neutral wire will be considered in detail in the further description.

4. Physical interpretation of the equivalent generalised circuit for 3-phase wye connected stator winding without neutral wire

Purely mathematical results obtained in previous section can be augmented with their physical interpretation.

Equation (13) is used to propose a 2-phase physical interpretation of the equivalent circuit for 3-phase machine with wye-connected stator winding without neutral wire. Its derivation is shown in Fig. 3. The first schema (Fig. 3a) is obtained by decomposition of the winding of phase *C* (Fig. 2c, flux linkage ψ_C, current $i_C = -(i_A + i_B)$) into two perfectly coupled fictitious coils (each with flux linkage ψ_C) connected in series with the phase *A* and *B* windings, respectively. These two fictitious coils have the same parameters (distribution, number of turns) like the phase winding *C*. In the resulting rearranged circuit, shown in Fig. 3b, these are merged with phase windings thus creating 2-phase generalised windings *AC* and *BC*.

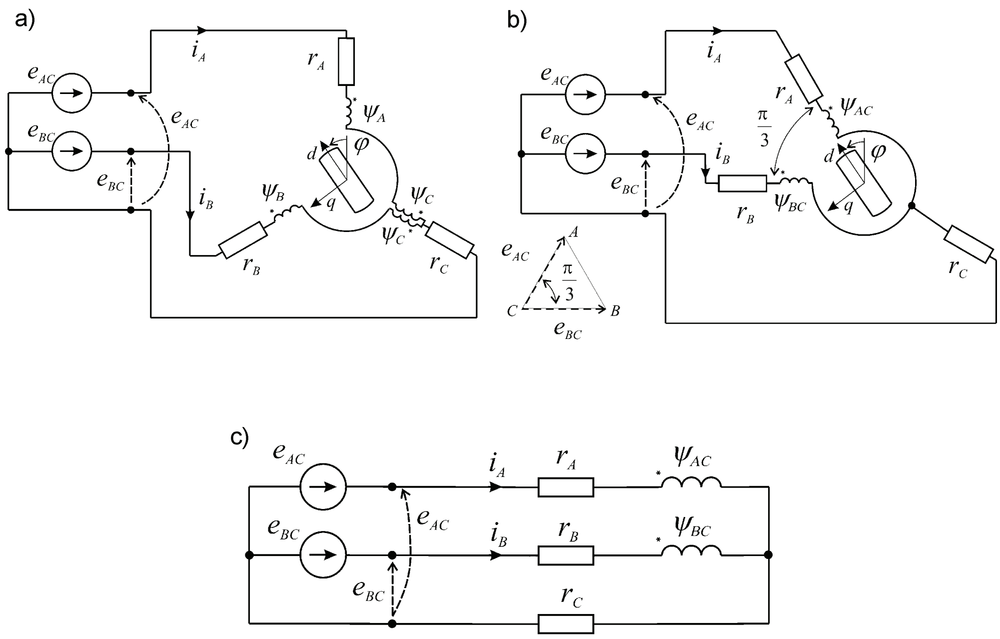

Fig. 3. Two-phase representation of reluctance motor a) decomposed *C* phase coil, b) phase windings rearranged into generalised windings, c) equivalent generalised circuit

The 2-phase generalised windings are galvanically connected by resistance r_c and their axes are rotated by π/6 in directions:

- anti-clockwise for the generalised winding *AC* relative to phase *A*,
- clockwise for the generalised winding *BC* relative to phase *B*.

The rotation is a result of geometric summation of the magnetomotive forces of coils containing both 2-phase generalised windings. Schema in Fig. 3b shows final position of the windings and triangle of supplying line-to-line voltages in which e_{AC} and e_{BC} are generalised external voltages in the circuit.

The terms *generalised windings* and *generalised circuit* (Fig. 3c) are used as these describe electric equations of HMEA.

The same result can be obtained with the help of separation principle [17] or u_s-shift (*voltage source*-shift) property [9], based on generalised Kirchhoff's laws.

5. Comparison of classical Lagrange actuator models and proposed HMEA – conclusions

To compare the proposed Hamiltonian approach with the classical Lagrange one the equation describing electric circuit is written in the classical form with currents as state variables which is derived from Lagrange equations (Fig. 4) [39]:

$$\frac{\mathrm{d}\boldsymbol{i}}{\mathrm{d}t} = \left(\boldsymbol{L}_d\left(\varphi,\boldsymbol{i}\right)\right)^{-1}\left(-\left(\omega\frac{\partial\,\boldsymbol{L}_n(\varphi,\boldsymbol{i})}{\partial\varphi}+\boldsymbol{R}\right)\boldsymbol{i}+\boldsymbol{u}\right), \tag{14}$$

where the following relationships hold:

$$\boldsymbol{L}_d\left(\varphi,\boldsymbol{i}\right) = \frac{\partial\boldsymbol{\Psi}(\varphi,\boldsymbol{i})}{\partial\boldsymbol{i}} = \left.\begin{bmatrix} \dfrac{\partial\psi_1}{\partial i_1} & \cdots & \dfrac{\partial\psi_1}{\partial i_N} \\ \cdots & \cdots & \cdots \\ \dfrac{\partial\psi_N}{\partial i_1} & \cdots & \dfrac{\partial\psi_N}{\partial i_N}\end{bmatrix}\right|_{\varphi=\mathrm{const}}, \tag{15}$$

$$\boldsymbol{\Psi}(\varphi,\boldsymbol{i}) = \boldsymbol{L}_n(\varphi,\boldsymbol{i})\boldsymbol{i}. \tag{16}$$

The main problem in successful implementation of the above equation is necessity of evaluation of dynamic inductance matrix which incorporates one nonlinear and N linear field solutions with “frozen reluctance value”. This process in extremely time-consuming [15, 30]. In equations (14) another differentiation with respect to angle is necessary, which can be very demanding when effects related to slotting are accounted for (like slot reluctance or cogging torques [24, 32]).

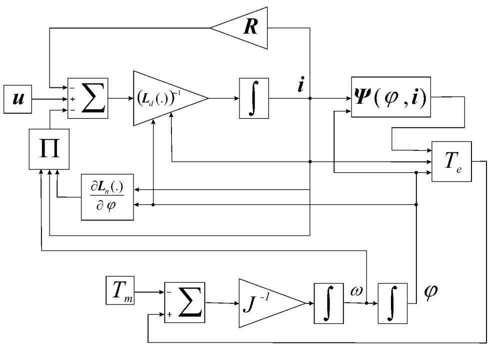

Fig. 4. Block diagram of an electromechanical actuator mathematical model using Lagrangian description ($(.) = (\varphi,\ \boldsymbol{i})$)

It must be underlined that in the HMEA there is no need for any differentiation in its electrical equations neither versus flux linkage nor versus angle (Fig. 1, Eq. (10)).

In the theory of electric machines a very important role play circuit models which can be called Simplified Lagrange models. In their development some additional assumptions are made in order to simplify the problem solution and make it more useful from practical point of view. Those assumptions are:

- decomposition of the magnetic field into main and leakage fluxes,
- assumption of sinusoidal spatial field distribution with only one or two space harmonics considered in the model [6, 25, 38],
- main magnetic flux paths are considered to saturate as a result of total MMF produced by all the machine windings,
- leakage magnetic flux paths of the windings are considered to saturate as a result of their individual MMF [38] or as non-saturated [6].

Either inductances [6] or co-energy based quantities [38] are used in the development of those models.

In Table 1 main properties of the three above described models:

a) Lagrange model,
b) Simplified Lagrange model,
c) HMEA which has two implementations:
   - with uniform databases [7, 8] – used as a reference model in the paper,
   - with triangulated databases – described in [P. I] of the current paper (with autonomous algorithm for electromagnetic torque evaluation),

are compared using the following criteria:

- main features of the model,
- properties of the model equations,
- possible practical applications.

Main conclusions can be summarised as follows.

- The most important advantage of the HMEA compared to Simplified Lagrange model is that magnetic field is analysed without decomposition into main and leakage fluxes as the model uses databases with global values of currents/flux linkages [7, 38]. It enables direct usage of data obtained using either FEM or measurement [26, 42]. Evaluation of energy/ /coenergy (Sec. 2.4 in [P. I]) and electromagnetic torque (Sec. 2.6 in [P. I]) is performed in the model using currents/flux linkage databases making the model self-contained,
- Another advantage of the HMEA compared to both Lagrange circuit models is that it is not necessary to calculate equivalent parameters (static and dynamic inductances, self and mutual inductances) which is extremely time-consuming in case of saturated core [15, 30].

The second conclusion is perhaps the most profound difference between Hamiltonian and Lagrangian approach to saturated electromechanical actuators.

6. Application of HMEA to an exemplary reluctance cageless motor

6.1. Description of numerical model

Data for the motor model presented in the whole paper were obtained with the help of the FEMM software (Fig. 5) [28]. Machine FE model was created for the prototype reluctance

Table 1. Comparison of electromechanical actuator models

Lp.	Main features of the model	Model: Lagrange	Model: Simplified Lagrange	Model: HMEA
1	Time necessary to create databases	VERY LARGE	MEDIUM / SMALL	LARGE / MEDIUM
2	Exact description of saturation	YES	NO	YES
3	Exact description of cogging/ ripple/reluctance (slotting) torque components	YES	NO	YES
4	Decomposition of the magnetic field into the main and leakage fluxes	NO	YES	NO
	Properties of the model equations			
1	Evaluation of equivalent parameters for solving the model equations	YES	YES	NO
2	Block diagram for integration of differential equations	VERY COMPLICATED (Fig. 4)	COMPLICATED	SIMPLE (Fig. 1)
3.	Evaluation time	VERY LONG	VERY SHORT	LONG (triangulated) / VERY SHORT (uniform)
	Possible practical applications			
1	Squirrel cage induction motors	NO	YES	NO
2	Synchronous reluctance motors SynRM (cageless)	YES	YES	YES
3	Switched reluctance motors	YES	NO	YES
4	Permanent magnet synchronous motors PMSM (cageless)	YES	YES	YES
5	Brushless direct current motors BLDC	YES	NO [32]	YES

machine using the stator of RSg 80-4A motor ($P_n = 0.37$ [kW], $I_n = 2.2$ [A], $2p = 4$ – number of poles, $Q_s = 36$ – number of stator slots) with the rotor lamination stack 72 [mm] long [8]. In numerical calculations the following discretisations were adopted [P. I]:

- for the angle: set $\Theta = \{0, 0.5,°..., 90°\}$ was employed ($K = 181$),
- for the phase current: series $I = \{-4, -3.5, ..., 4\}$ [A] was used which defines the current set I^k as a Cartesians product $I^k = I \times I$, $P(k) = 17^2$.

Exemplary results of field calculations are shown in (Fig. 5).

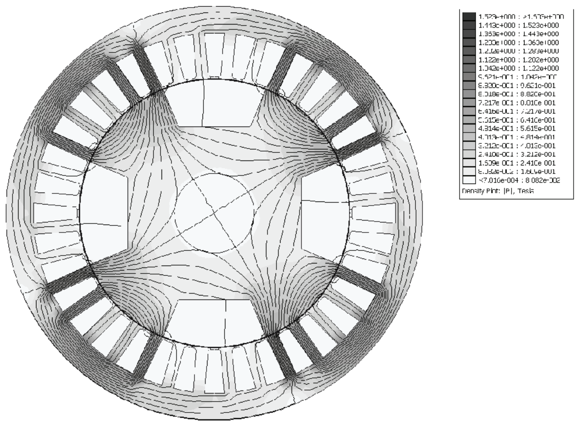

Fig. 5. Magnetic field distribution in reluctance motor two-dimensional FEM model (angle $\varphi = 45°$, currents $i_A = 1$ [A], $i_C = i_B = -0.5$ [A])).

In Table 2 a comparison between uniform and triangulated databases used in different implementations of HMEA is presented. Main problem of uniform databases is clearly visible – incorrect description of saturation phenomenon in highly saturated regions [7].

Table 2. Uniform/Triangulated databases for $\varphi = \varphi_1$

Uniform DATABASE	Triangulated DATABASE
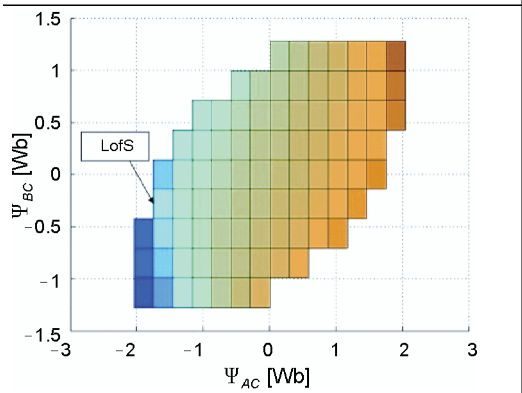	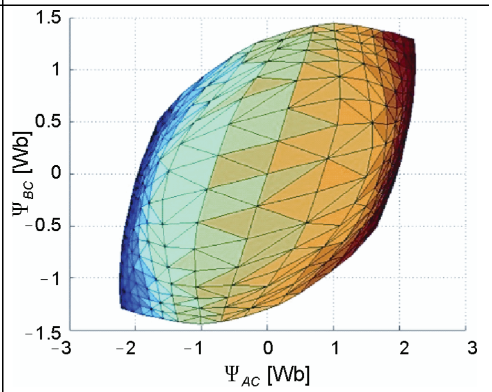
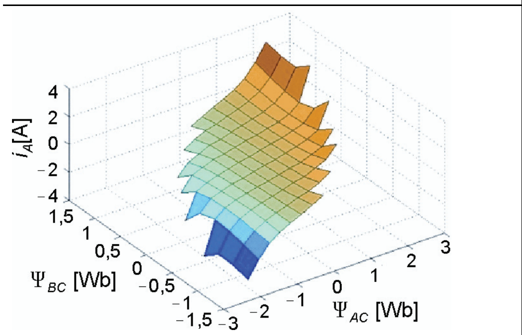	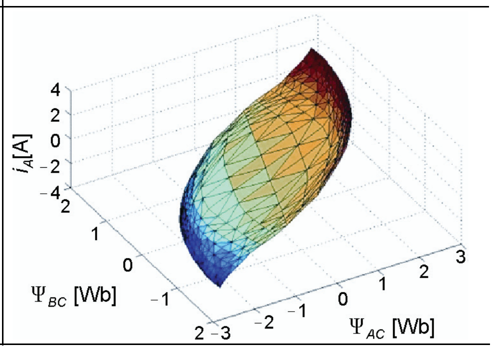

6.2. Simulation results for φ = const

Numerical simulations in Matlab/SIMULINK were performed for 3-phase symmetrical phase voltages of magnitude U_{ph} = 30 [V] / 60 [V], frequency f = 10 [Hz], $\varphi(t) = 0$, $\omega(t)$ = = 0 [rad/s] for initial conditions: $\psi_{AC}(0) = \psi_{BC}(0) = 0$ [Wb]. Remaining model parameters are: r_f = 13 [Ω] – phase resistance, J = 0.01 [kg·m^2], T_m = 0 [N·m]. Simulation time in Matlab/ /SIMULINK is 1 [s].

Results in Table 3 show that compatibility of results between different implementations of HMEA (reference & proposed) both for current and torque is very good. To enable better verification enlarged figures were added showing 0.25 [s] of the waveforms. It is especially important in case of torque as values for proposed model are internally evaluated using algorithm described in [P. I] while in case of reference model values were obtained using approximation of FEM data. Furthermore the proposed model overcame the main drawback of the reference model related to limited database range often resulting in Loss of Stability due to overflow (LofS., Table 2, Table 3) [7].

Table 3. Comparison of simulation results for $\varphi = \varphi_1$

U_{ph} = 30 [V]	U_{ph} = 60 [V]
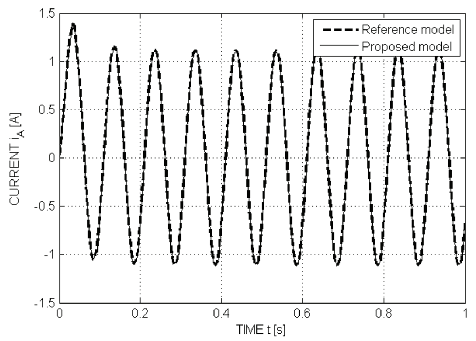	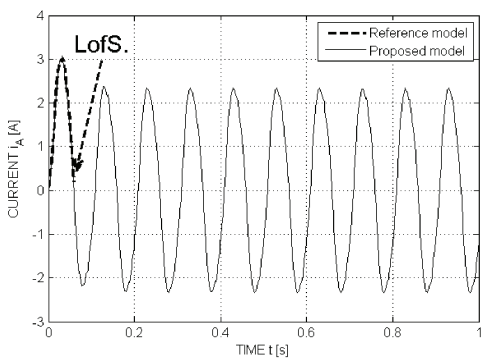
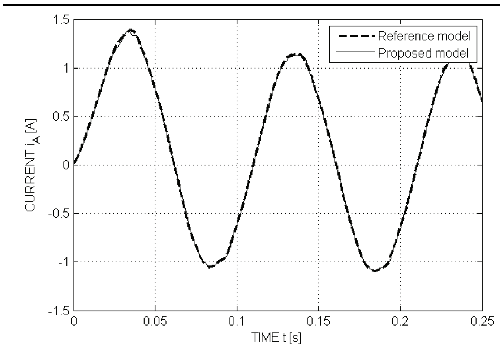	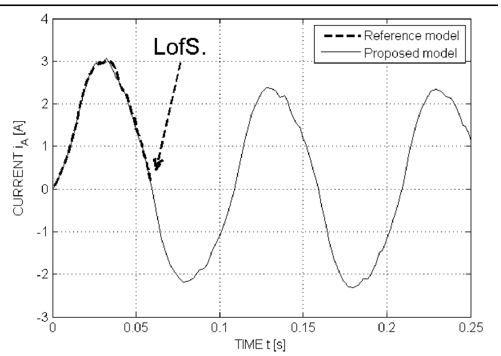

U_{ph} = 30 [V]	U_{ph} = 60 [V]

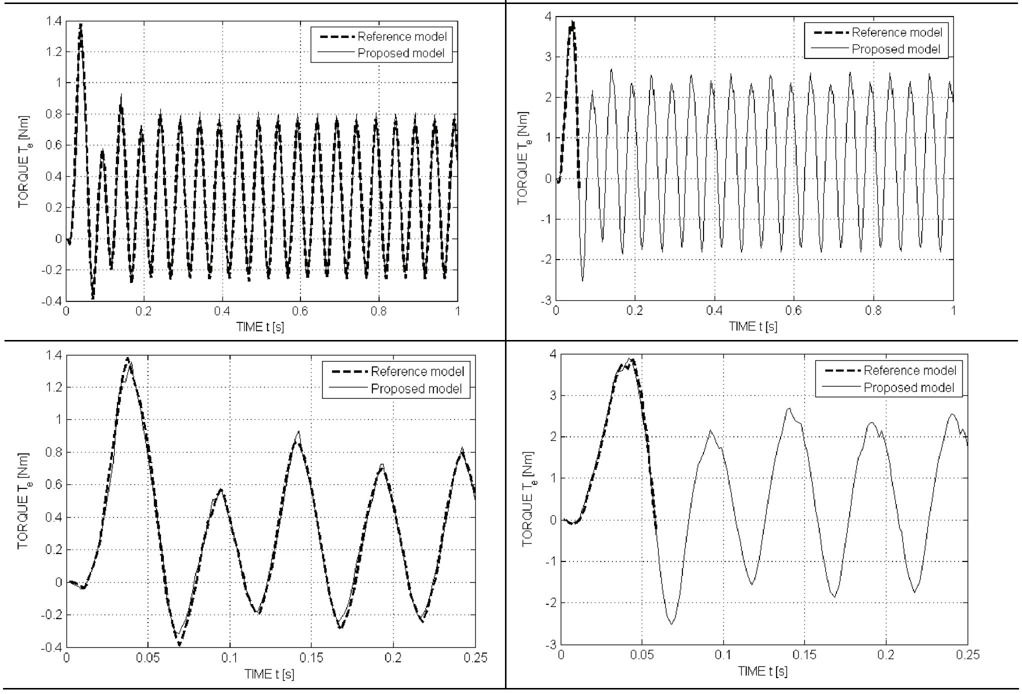

There is, unfortunately, also one important disadvantage of the proposed HMEA implementation. Evaluation time is much longer compared to the reference one (Table 4, Table 6) [8]. The reason for this problem is poor computation speed which can be achieved using TriRep/DelaunayTri structures compared to Lookup Tables used for interpolation in case of reference implementation [2, 27].

Though it must be underlined that the reference HMEA implementation is based on pure interpolation of uniform databases while the proposed HMEA implementation with triangulated databases enables independent evaluation of torque making it self-contained.

Table 4. Evaluation time [s] for $\varphi = \varphi_1$

Model	Reference	Proposed
30 [V]	0.4	64
60 [V]	overflow	74

6.3. Simulation results for ω = const

Numerical simulations in Matlab/SIMULINK were performed for 3-phase symmetrical phase voltages of magnitude U_{ph} = 30 [V], frequency f =10 [Hz] for initial conditions: $\varphi(t)$ = 0, $\psi_{AC}(0)$ = $\psi_{BC}(0)$ =0 [Wb]. Two speed values were verified $\omega = \omega_s$, $\omega = -\omega_s$ where

$\omega_s = 2\pi f / p$ [rad/s] (synchronous speed). Remaining model parameters were as in Sec. 6.2. Fourier harmonic analysis (Table 7) was applied to the last period of the waveforms which can be regarded as steady state operation.

Results in Table 5 and Table 7 show that proposed HMEA properly describes:

- slot effects evident in plots for $\omega = \omega_s$ (torque harmonic $f_T = (Q_s/p) f = 180$ [Hz] in Table 7),
- appearance of additional component of frequency $f_3 = 3f = 30$ [Hz] in current waveform which is evident in plots for $\omega = -\omega_s$ (current harmonics in Table 7) [34].

Table 5. Comparison of simulation results for ω = const

$\omega = \omega_s$	$\omega = -\omega_s$
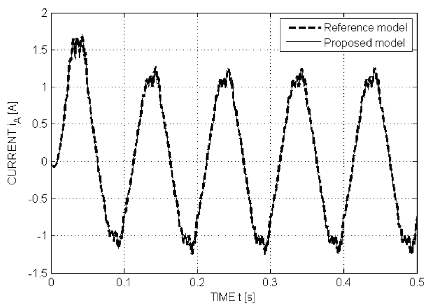	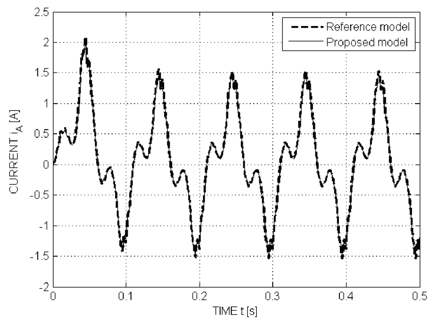
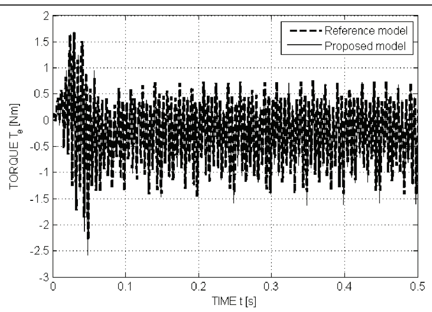	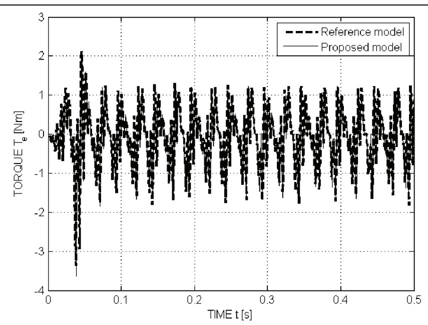

Table 6. Evaluation time [s] for ω = const

Model	Reference	Proposed
$\omega = \omega_s$	0.8	110
$\omega = -\omega_s$	0.85	120

7. General remarks

In the formulation of the HMEA only two assumptions were made:

- eddy currents are neglected,
- hysteresis phenomenon is neglected,

necessary to apply Hamiltonian state-space description [37]. No other assumptions traditionally used in circuit models of electromechanical actuators are necessary [25, 39].

Therefore, in the HMEA it is possible to account simultaneously for the following phenomena:

- saturation effect,
- MMF harmonics,
- slotting of magnetic cores [24],
- cogging effect (when applied to BLDC/PMSM [32]).

Table 7. Harmonic analysis of results for ω = const

$\omega=\omega_s$	$\omega=-\omega_s$
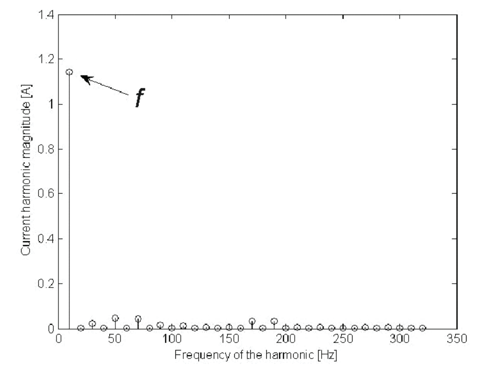	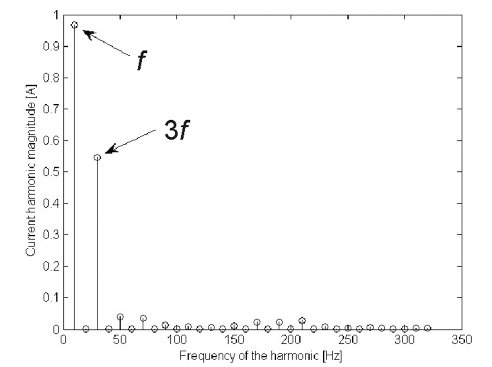
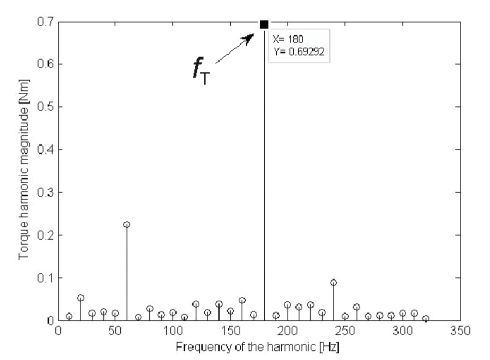	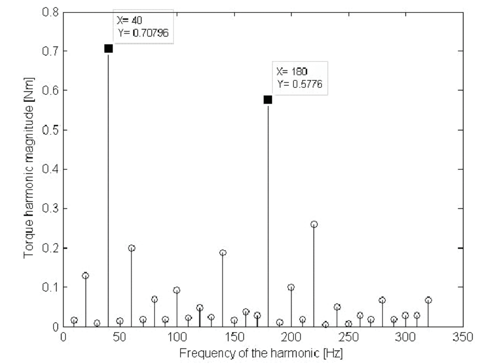

Above mentioned capabilities of proposed HMEA implementation are based on assumed topology of databases (local linear homeomorphism [19, 40]). Similar approach has been used in description of electronic nonlinear circuits and networks for decades [41]. To apply this approach for electromechanical actuators one must use proper current sets I^k, $k \in \{1, \ldots, K\}$ to ensure that local behaviour of analysed variables can be treated as linear. The solution of this problem could be found in procedures used in Finite Element Analysis FEA [29]. Initially sets I^k could be quite coarse and then – based on the shape of obtained hypersurfaces (Tables 5, 6 in [P. I]) – additional points could be introduced in order to increase accuracy of representation of saturation phenomena. That procedure would be quite similar to mesh refinement in FEA [29]. TriRep/DelaunayTri structures in Matlab are capable of such changes in the data [27]. Their drawback is speed which results in much longer evaluation time compared to uniform database (Table 4, Table 6). This problem could be solved in the future when full parallel algorithm using CUDA (Compute Unified Device Architecture) technology for Graphic Processor Units GPU NVIDIA is applied (due in Matlab relase 2010b) [45].

Another possibility which can be applied in the model is application of higher-order polynomial interpolation which is also extensively employed in FEA [29]. However that would lead to loss of local invertibility of approximations f_A^k / f_A^{-k} which is the basis of the proposed approach [P. I] [19].

Presented results show that the following issues need further investigation:

- optimisation of algorithm time performance (e.g. CUDA technology),
- comparison of different algorithms of torque calculations [1, 11, 13, 29]:
  – employment of methods based on energy and coenergy,
  – global Fourier series/FFT for coenergy as data obtained using FEM allow to create a uniform database thus enabling off-line evaluation of Fourier series coefficients in the vertices of triangulation $T^k(I^k, \boldsymbol{IK}^k)$ as it would be the same for any k [P. I],
- determination of measurement procedure for database identification [26, 42].

Electromagnetic torque evaluation using Fourier series / FFT would be similar to methods used in standard analysis of electromechanical actuators [4, 25, 37, 39].

References

[1] Arkkio A., Hannukainen A., Niemenmaa A. *Power balance for verifying torque computation within time-discretized finite-element analysis.* XXI Symposium Electromagnetic Phenomena in Nonlinear Circuits EPNC'2010, Germany, Dortmund and Essen, pp.23-24.

[2] Agoston M.K., *Computer graphics and geometric modeling – mathematics.* Springer 2005.

[3] Boldea I. Nasar S.A., *Electric drives.*Taylor&Francis (2005).

[4] Boldea I., *Reluctance synchronous machines & drives.* Oxford Univ. Press (1996).

[5] Borsuk K., *Multidimensional analytical geometry.* PWN, Warsaw (1977) (in Polish).

[6] Brown J.E., Kovacs K.P., Vas P., *A method of including the effects of main flux path saturation in generalised equations of A.C. machines.* IEEE Transactions on Power Apparatus and Systems PAS-102(l): 96-103 (1983).

[7] Burlikowski W., *Mathematical model of an electromechanical actuator using flux state variables applied to reluctance motor*, COMPEL 25(1): 169-180 (2006).

[8] Burlikowski W., *Influence of saturation modelling method on results obtained using different implementations of reluctance motor simulational model.* XX Symposium Electromagnetic Phenomena in Nonlinear Circuits EPNC'2008, France, Lille, pp. 69-70 (2008).

[9] Chua L.O., Desoer C.A., Kuh E.S., *Linear and nonlinear circuits.* McGraw-Hill (1987).

[10] Chua L.O., McPherson J.D., *Explicit topological formulation of lagrangian and Hamiltonian equations for nonlinear networks.* IEEE Transactions on Circuits and Systems CAS-21(2): 277-286 (1974).

[11] Coulomb J.I., *A methodology for determination of global electromechanical quantities from a finite element analysis and its application to the evaluation of magnetic forces, torques and stiffness.* IEEE Trans. Magn. 19: 25 14-25 19 (1983).

[12] De Berg M., Van Kreveld M., Overmars M., Schwarzkopf O., *Computational Geometry.* Springer (2000).

[13] Demenko A. *Movement Simulation in Finite Element Analysis of Electric Machine Dynamics*, IEEE TRANSACTIONS ON MAGNETICS, VOL 32. NO 3, MAY 1996, pp. 1553-1556.
[14] Demenko A. *Time-Stepping FE Analysis of Electric Motor Drives with Semiconductor Converters*, IEEE TRANSACTIONS ON MAGNETICS, VOL. 30, NO. 5, SEPTEMBER 1994, pp. 3264-3267.
[15] Demenko A. , Hameyer K. *Field and Field-Circuit Description of Electrical Machines*, Proc. of EPE-PEMC 2008, pp. 2412-2419.
[16]Engelking R., Sieklucki K., *Introduction to topology*, (in Polish), PWN, 1986.
[17] Fryze S. *Selected problems of theoretical basis of electrical engineering*, (in Polish), PWN, Warsaw-Wrocław,1966.
[18] Goodman J.E., O'Rourke J., et al. *Handbook of discrete and computational geometry.* CRC Press (1997).
[19] Groff R.E., *Piecewise linear homeomorphisms for approximation of invertible maps.* Ph.D. Thesis, Univ. of Michigan (2003).
[20] Hu, Y., Torrey, D.A., *Study of the mutually coupled switched reluctance machine using the finite element-circuit coupled method.* IEE Proceedings – Electric Power Applications 149(2): 81-86 (2002).
[21] Jagieła M., Grabiec T., *Coupling electromagnetic (FE) models to multidomain simulator to analyse eletrical driver and complex control systems.* AEE 59(3-4): 189-201 (2010).
[22] Jeltsema D., Scherpen J.M.A., *Multidomain modeling of nonlinear networks and systems.* IEEE Control Systems Magazine, August, pp. 28-59 (2009).
[23] Kang S.M., Chua L.O., A global representation of multidimensional piecewise-linear functions with linear partitions. IEEE Transactions on Circuits and Systems CAS-25(11): 938-940 (1978).
[24] Kluszczyński K., Spałek D., *Step-by-step analysis of induction machines allowing for slotting.* Polish Society for Theoretical and Applied Electrical Engineering, Warsaw (2002).
[25] Krause P., *Analysis of electric machinery.* McGraw-Hill (1986).
[26] Ludwinek K., Siedlarz A., *Harmonic distortion analysis in armature currents of synchronous machine during co-operation with the power system*. Zeszyty Problemowe Maszyny Elektryczne 84: 217-223 (2009).
[27] *Matlab on-line Manual*, R2010a, 2010.
[28] Meeker D., *Finite element method magnetics.* User's Manual, Ver. 4.2 (2007).
[29] Meunier G., et al., *The finite element method for electromagnetic modelling.* ISTE Ltd (2008).
[30] Nehl T.W., Fouad F.A., Demerdash N.A., *Determination of saturated values of rotating machinery incremental and apparent inductances by an energy perturbation method.* IEEE Transactions on Power Apparatus and Systems PAS-101(11): 4441-4451 (1982).
[31] Nowak, L., *Dynamic operation of an electromechanical actuator,* COMPEL18(4): 611-618 (1999).
[32] Ozturk S.B., Toliyat H.A., *Sensorless direct torque and indirect flux control of brushless DC motor with non-sinusoidal back-EMF.* Proc. IEEE-IECON Annu. Meeting, Orlando, pp. 1373-1378 (2008).
[33] Park R.H., *Two-reaction theory of synchronous machines – generalized method of analysis – Part I.* AIEE Trans. 48:716-727 (1929).
[34] Paszek W., *Dynamics of alternating current electric machines.*, Helion, Gliwice (1998) (in Polish).
[35] Puchała A., *Dynamics of machines and electromechanical systems.*, PWN, Warsaw (1977) (in Polish).
[36] Schlensok Ch., Henneberger G., *Simulation of a PMSM with SIMPLORER-FLUX2D-Coupling.* CD-ROM Proc. of XVth ICEM'2002, Brugge-Belgium, August (2002).
[37] Schmitz N.L., Novotny D.W., *Introductory electromechanics*. The Ronald Press Company, New York (1965).
[38] Sobczyk T.J., *Inductanceless model of salient-pole synchronous machines.* Proc. of SPEEDAM, pp. 620-625 (2008).
[39] Sobczyk T.J., *Methodological aspects of mathematical modeling of induction machines.* WNT, Warsaw (2004) (in Polish).
[40] Spanier E.H., *Algebraic topology*. McGraw-Hill Series in Higher Mathematics (1972).

[41] Stern T.E., *Piecewise-linear network theory.* MIT, Research Laboratory of Electronics, Technical Report 315 (1956).
[42] Stumberger G., Stumberger B., Dolinar D., *Identification of linear synchronous reluctance motor parameters.* IEEE Transactions On Industry Applications 40(5): 1317-1324 (2004).
[43] Wach P., *Devices for electromechanical energy conversion.* Opole (1991) (in Polish).
[44] Zomorodian A.J., *Topology for computing.* Cambridge Monographs on Applied and Computational Mathematics (2005).
[45] Zunoubi M.R., Payne J., Roach W.P., *CUDA Implementation of TEz-FDTD solution of Maxwell's equations in dispersive media.* IEEE Antennas and Wireless Propagation Letters 9: 756-759 (2010).
[P. I] Part I of the paper.